ENGLISH VERSION

# Shear behavior of CFRP - reinforced concrete beams using FEM

## Comportamiento cortante de vigas de hormigón reforzadas con CFRP utilizando el MEF

A. K. Sakban [1]*, A. Mashrei ** http://orcid.org/0000-0002-5909-756X

* Misan University – Misan, IRAQ
** Thi-Qar University – Nasiriya, IRAQ

Fecha de Recepción: 05/06/2020
Fecha de Aceptación: 10/12/2020
PAG 117-141

***Abstract***

*In the current study, the finite element method using the ABAQUS program is employed to investigate the shear behavior of reinforced concrete (RC) beams strengthened by carbon fiber reinforced polymer CFRP. Load-deflection curves, modes of failure and the pattern of the cracks are studied. Also, the influence of compression strength of concrete, the configuration of CFRP (U shape and 2 side bond shape) and shear span to depth ratio (a/h ratio). The results show that the shear capacity of RC beams strengthened by CFRP increased by a maximum percentage of up to 111.7% compared to the unstrengthened beam. Also, it is found that by increasing the compressive strength of concrete from 40 MPa to 65 MPa the load-carrying capacity increases by 28% and the stiffness also increased, while the decrease of shear span to depth ratio from 1.66 to 2.33 leads to increasing the shear capacity by 23%. The maximum load of beam strengthened with U shape increased by up to11.5% when compared with the same beam strengthened with two side bond shapes of CFRP. However, the gain in the strength was reached to 22.7% for beams strengthened with CFRP laminate compare to unstrengthened beams. The strengthening of RC beams by CFRP laminates using the near surface mounted (NSM) technique is more efficient than the externally bonded reinforcement (EBR) technique for all beams in the shear behavior. The finite element models provide a good level of accuracy compared to experimental results and ACI-440.*

***Keywords:*** *FEM, CFRP, behavior, shear, beam*

**Resumen**

En el presente estudio se emplea el método de elementos finitos utilizando el programa ABAQUS para investigar el comportamiento cortante de vigas de hormigón armado (RC), endurecidas con polímero reforzado con fibra de carbono CFRP. Se estudian las curvas carga-deflexión, los modos de fallo y el patrón de las grietas. También se estudia la influencia de la resistencia a la compresión del hormigón, la configuración del CFRP (forma de U y forma unión de 2 lados) y la relación entre la luz de corte y la profundidad (relación a/h). Los resultados muestran que la capacidad de corte de las vigas de CR reforzadas con CFRP aumentó en un porcentaje máximo de hasta el 111,7% en comparación con la viga no reforzada. Además, se observa que al aumentar la resistencia a la compresión del hormigón de 40 MPa a 65 MPa, la capacidad de carga se incrementa en un 28% y la rigidez también aumenta, mientras que la disminución de la relación entre la luz de corte y la profundidad de 1,66 a 2,33 conduce a aumentar la capacidad de corte en un 23%. La carga máxima de la viga reforzada con forma de U aumentó hasta un 11,5% en comparación con la misma viga reforzada con dos formas de unión lateral de CFRP. Sin embargo, la ganancia en la resistencia fue del 22,7% para las vigas reforzadas con laminado de CFRP en comparación con las vigas no reforzadas. El refuerzo de las vigas de hormigón armado con laminados de CFRP mediante la técnica de montaje en superficie (NSM), es más eficaz que la técnica de refuerzo de unión externa (EBR), para todas las vigas en el comportamiento cortante. Los modelos de elementos finitos proporcionan un buen nivel de precisión en comparación con los resultados experimentales y la norma ACI-440.

**Palabras clave:** FEM, CFRP, comportamiento, cortante, viga

## *1. Introduction*

*Reinforced concrete (RC) structural elements such as beams may be subjected to significant shear stresses. Upgrading or strengthening becomes necessary when these structural elements are not able to provide satisfactory strength and serviceability. Shear failure of RC beams could occur without any warning. Many existing RC members are found to be deficient in shear strength and need to be repaired. Shear deficiencies in reinforced concrete beams may occur due to many factors such as inadequate shear reinforcement, reduction in steel area due to corrosion.*

*In general, shear resistance of RC beams has been increased when strengthed by CFRP against shear failure using NSM and EBR techniques. FRP composites are lightweight, non-corrosive, and easily constructed which exhibit strength and high specific stiffness. FRP composites have been used in rehabilitation and new construction structures, and external reinforcement for seismic upgrade and strengthening.*

*Maney experimental researches have investigated the effect of strengthening RC beams by CFRP laminate or sheet on the shear strengrth. However, some of the numerical studies were used to represent RC beams strengthed by CFRP as in. Accordingly, most of the previous works related to the strengthening of concrete beams by CFRP to enhance the shear behavior of RC beams were experimental studies. It is very essential to understand the behavior of CFRP-RC beams by presenting more theoretical and numerical studies. The theoretical works related to the behavior of RC beams with CFRP in shear using program ABAQUS are still limited.*

[1] ***Corresponding author:***
*Misan University – Misan, IRAQ*
*E-mail: nmnm2178@gmail.com*

*In this study, finite element analysis using ABAQUS program was presented to investigate the efficiency of using CFRP with NSM or EBR technique to enhance the shear strength of RC beams. The FEM model was build based on the experimental results concluded by (Barros et al, 2007). A parametric study was presented to investigate the impact of different parameters on the shear strength of RC beams strengthened by CFRP.*

## 2. Materials and methods

### 2.1 Materials

*The same properties of steel reinforcement and concrete proposed by (Barros et al., 2007) have been used in the current study. (Table 1) shows the properties of steel and concrete materials.*

*Two types of CFRP were used in this paper: the first type is CFRP sheets with 80 mm in width used for the flexural strengthening. The second type is CFRP- laminates with 1.4 x 9.6 mm2 as a cross-sectional area in the flexural strengthening. The properties of the CFRP used in this study are listed in (Table 2).*

***Table 1.*** *Properties of steel bars and concrete*

| ***concrete*** $f'_c$ ***(MPa)*** | ***steel*** | | |
|---|---|---|---|
| | $\emptyset_s$ ***(mm)*** | ***(MPa)*** $f_y$ | $f_u$ ***(MPa)*** |
| *49.2*[a] | *6 (stirrups)* | *540* | *694* |
| | *6 (long.)* | 622 | 702 |
| | | 618 | 691 |
| *56.2*[b] | *10* | *464* | *581* |
| | *12* | *574* | *672* |
| | | *571* | *673* |

a: A series.
b: B series.

***Table 2.*** *Properties of the CFRP and adhesive materials*

| **Material** | **Young's modulus (GPa)** | **Tensile strength (Mpa)** | **Ultimate strain (%)** | **Thickness (mm)** |
|---|---|---|---|---|
| sheet | 390 | 3000 | 0.8 | 0.167 |
| epoxy | 3 | 54 | 2.5 | ---- |
| primer | 12 | 0.7 | 3 | ---- |
| Adhesive | 5 | 16-22 | ---- | ---- |
| Laminate | 166 | 2286 | 1.3 | 1.4 |

## 3. Finite element analysis

*The finite element method (FEM) was performed to model the nonlinear behavior of RC beams strengthened by CFRP.*

### 3.1 Concrete

*The plastic damage was performed to model the concrete behavior. This model assumes that the major two failure modes of concrete are tensile cracking and compression failure as shown in (Figure 1). The modulus of elasticity ($E_c$) and modulus of rupture were calculated theoretically based on experimental values of compressive strength of concrete ($f'_c$).*

*For tension behavior (Equation 1):*

$$f_t=0.61\sqrt{f'_c} \quad (1)$$

*(Equation 2)*

$$E_c=22\,(0.1 * f'_c)^{0.3}\,1000 \quad (2)$$

$\in$=0.000117

*(Equation 3)*

$$\in_{et}=\in_t= f_t/E_c \quad (3)$$

*(Equation 4)*

$$\sigma_t = f_t(\in_t/\in)^{0.4} \quad (4)$$

*(Equation 5)*

$$\in_{cst}=\in_t-\left(\frac{\sigma}{E_c}\right) \quad (5)$$

*For compressive behavior:*

*(Equation 6)*

$$k = 1.05 * E_c\left(\frac{\in_{c1}}{f_{\bar{c}}}\right) \quad (6)$$

*(Equation 7)*

$$\in_{c1}= 0.0014(2 - e^{0.024*f'_c} - e^{0.14\,f'_c}) \quad (7)$$

*(Equation 8)*

$$\aleph = \in c_{ii}/\in_{c1} \quad (8)$$

*(Equation 9)*

$$\sigma_c = f'_c * \left(\frac{k*\aleph-\aleph^2}{1+(k-2)*\aleph}\right) \quad (9)$$

*where:*

$f_t$*: tensile strength of concrete,* $f'_c$ *: compressive strength of concrete,* $E_c$*: elastic modulus,* $\in_t$*: strain in the tension zone,* $\sigma_t$*: tensile stress in plastic range,* $\in_{cst}$*: tensile strain in the plastic range,* $\in_{c1}$*: strain at the peak stress,* $\sigma_c$*: compressive strength of concrete in plastic range.*

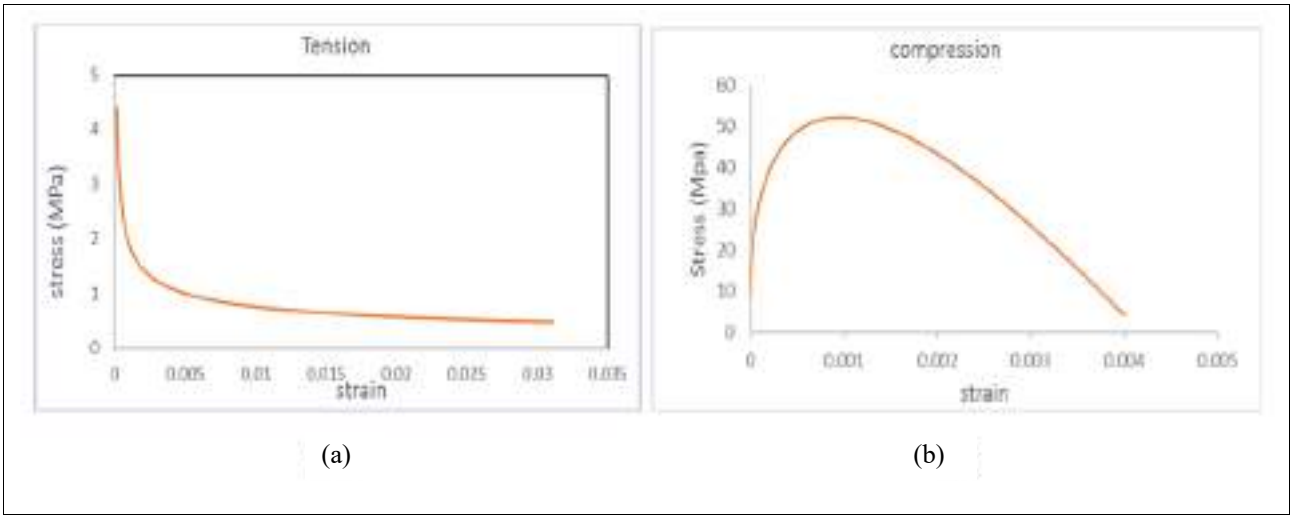


***Figure 1.*** *Stress-strain curves of concrete a) tension b) compression (CEN. European Committee for Standarization, 2014)*

### *3.2 Steel reinforcement*

*The steel reinforcement was used as an elastic-plastic material. (Figure 2) shows the stress-strain relationship of steel in compression and tension behavior. The elastic modulus and the yield stress were obtained from the experimental work conducted by Barros et al, 2007. A Poisson's ratio used in this study equal to 0.3 for the steel reinforcement. A perfect bond between concrete and steel was assumed.*

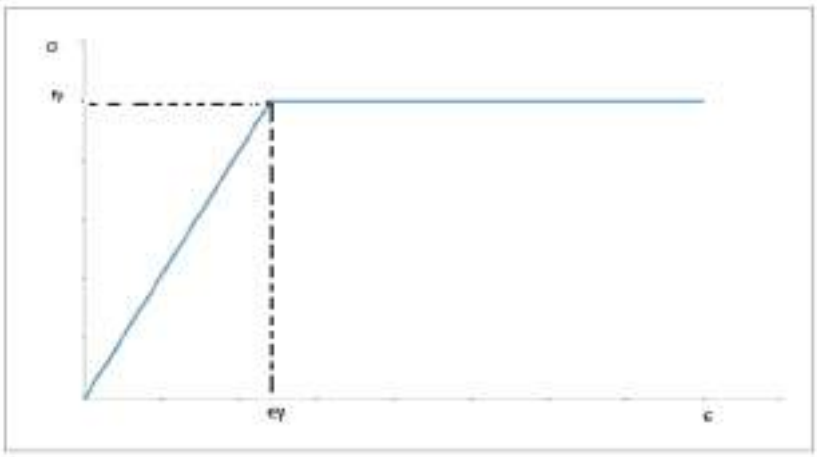


***Figure 2.*** *Stress-strain relationship of steel reinforcement in tension and compression*

### *3.3 CFRP*

*Generaly two models were used to represent CFRP. Firstly, CFRP was assumed as a linear elastic isotropic until failure. While in another model, CFRP was assumed as a linear elastic orthotropic material. The first model has been used in this study. The CFRP properties were specified by the manufacturer. A Poisson's ratio of 0.3 was used for CFRP. The stress-strain of CFRP is shown in (Figure 3).*

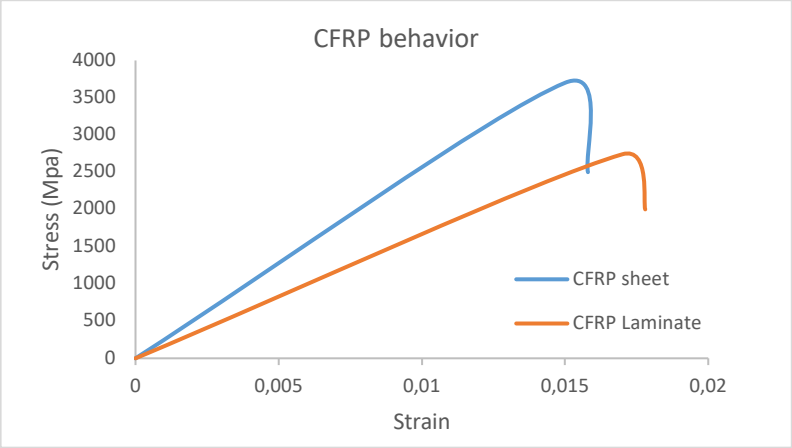


***Figure 3.*** *Stress-strain curve of CFRP for sheet and laminate types*

### *3.4 CFRP–concrete interface*

*Two models were utilized to model the interface between CFRP concrete surfaces A perfect bond was assumed in the first model and a cohesive model was assumed in the second one. (Figure 4) shows the relationship between maximum shear stress ($\tau_{max}$) and effective opening displacement ($\delta$) in the interface zone between concrete and CFRP by using simple bilinear traction–separation law. The interface is modeled with a small thickness and the initial stiffness $K_0$ is defined as (Guo et al., 2005) (Equation 10)*

$$k_0 = \frac{1}{\frac{t_i}{G_i}+\frac{t_c}{G_c}} \quad \text{.....(10)}$$

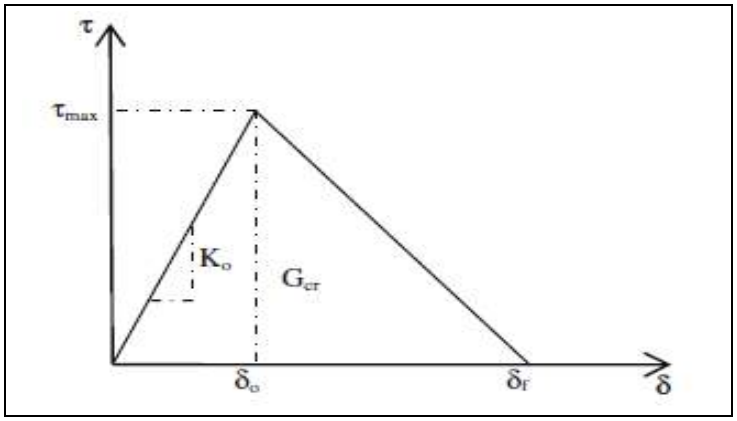


***Figure 4.*** *Bilinear traction–separation constitutive law*

*It is assumed that $G_i$= 0.665 GPa, $G_c$ = 10.8 GPa, $t_i$ = 0.5 mm, and $t_c$ = 5 mm. The relation between the effective opening displacement and traction stress is represented by the stiffness ($K_0$), opening displacement at fracture ($\delta_f$), the material strength ($\tau_{max}$) and the energy required to open the crack ($G_{cr}$) which is defined by the area under the traction–displacement relationship as shown in (Figure 4).(Equation 11) (Equation 12), provides an upper limit of the maximum shear stress. ($t_{max}$,):*

$$t_{max} = 1.5\, Bw\, f_t \quad \text{.....(11)}$$

*where:*

$$Bw = \sqrt{\frac{2.25-\frac{bf}{bc}}{1.25+\frac{bf}{bc}}} \quad \text{.....(12)}$$

*The value of fracture energy ($G_{cr}$) was ranged between 300 J/m2 and 1500 J/m$^2$ as assumed in other researches. The value of 900 J/m$^2$was used in current research.*

*The damage was assumed to occur firstly when the nominal stress ratios reached value one this criterion can be represented by (Equation 13)(Hibbitt and Sorensen, 2000):*

$$(\sigma_n/\sigma^\circ_n)^2 + (t_s/t^\circ_s)^2 + t_t/t^\circ_t)^2 \quad = 1 \quad \text{.....(13)}$$

***$\sigma^\circ_n$ = $f_t$ =4.4 MPa, and $t^\circ_s$ = $t^\circ_t$ = 1.5** MPa, used in this study*

## 4. Shear strengthening

*Numerical modeling to study the behavior of beam strengthened for shear by CFRP under four-point loading using the ABAQUS program using the experimental work conducted by (Barros et al., 2007) to build the model. The numerical study has been adopted based on the experimental study of four series of tested beams presented by (Barros et al., 2007). (Figure 5) and (Table 3) show the support conditions, reinforcement arrangement, and geometry of the beams. Each series was composed of a beam without shear reinforced (R) and the following beams strengthed with shear reinforcing: strips of CFRP sheet (M), steel stirrups (S), strips of CFRP at 450_ with the beam longitudinal axis (IL) and laminate strips of CFRP at 900_ with the beam longitudinal axis laminate (VL).*

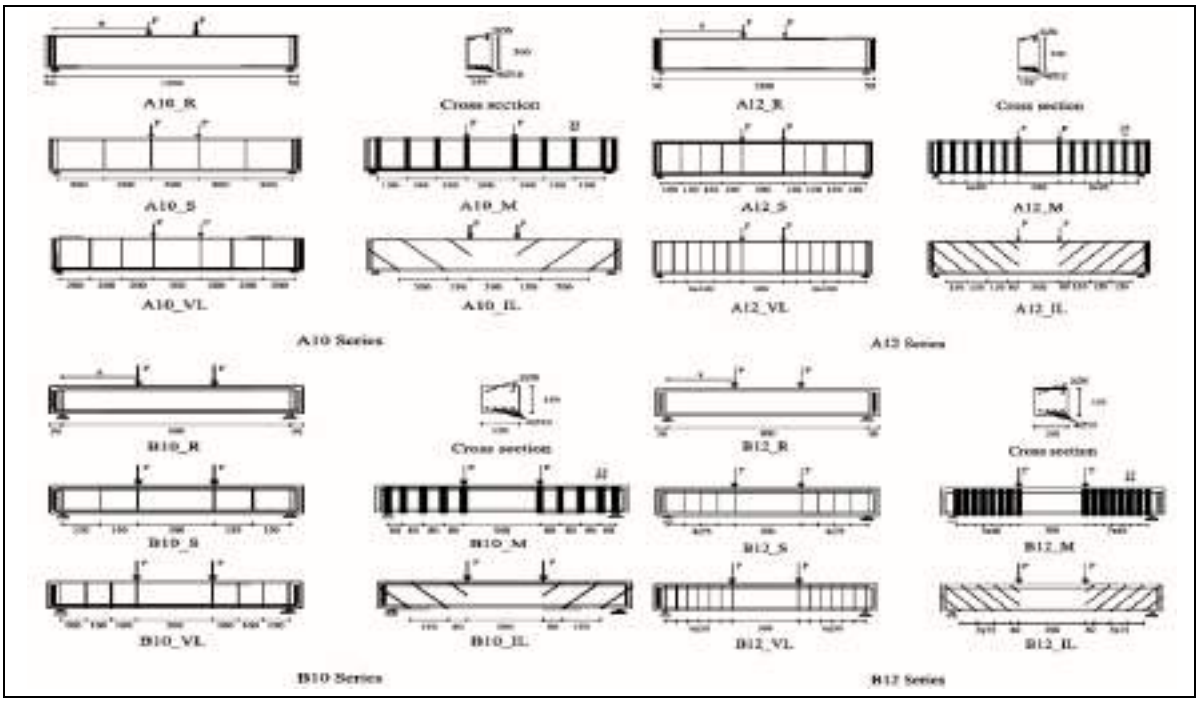


***Figure 5.** Series of beams strengthened for the shear (dimensions in mm)*

***Table 3.*** *Series beams strengthened for the shear*

| Beam designation | | | Shear strengthening systems | | | |
|---|---|---|---|---|---|---|
| | | | Material | Quantity | Spacing (mm) | Angle (°) |
| A series | A10 seies | A10-R | ----- | ----- | ------ | ------ |
| | | A10-S | Steel stirrups | 6Ø6 of two branches | 300 | 90 |
| | | A10-M | CFRP sheet | 8*2 layers of 25 mm (U shape) | 190 | 90 |
| | | A10-VL | CFRP laminate | 16 CFRP laminates | 200 | 90 |
| | | A10-IL | CFRP laminate | 12 CFRP laminates | 300 | 45 |
| | A12 series | A12-R | ----- | ----- | ------ | ------ |
| | | A12-S | Steel stirrups | 10Ø6 of two branches | 150 | 90 |
| | | A12-M | CFRP sheet | 14*2 layers of 25 mm (U shape) | 95 | 90 |
| | | A12-VL | CFRP laminate | 28 CFRP laminates | 100 | 90 |
| | | A12-IL | CFRP laminate | 24 CFRP laminates | 150 | 45 |
| B series | B10 seies | B10-R | ----- | ----- | ------ | ------ |
| | | B10-S | Steel stirrups | 6Ø6 of two branches | 150 | 90 |
| | | B10-M | CFRP sheet | 10*2 layers of 25 mm (U shape) | 80 | 90 |
| | | B10-VL | CFRP laminate | 16 CFRP laminates | 100 | 90 |
| | | B10-IL | CFRP laminate | 12 CFRP laminates | 150 | 45 |
| | B12 series | B12-R | ----- | ----- | ------ | ------ |
| | | B12-S | Steel stirrups | 10Ø6 of two branches | 75 | 90 |
| | | B12-M | CFRP sheet | 16*2 layers of 25 mm (U shape) | 40 | 90 |
| | | B12-VL | CFRP laminate | 28 CFRP laminates | 50 | 90 |
| | | B12-IL | CFRP laminate | 24 CFRP laminates | 75 | 45 |

## *5. Results and discussion*

### *5.1 Load-deflection curve*

*This section discusses the ultimate load and the relationship between load and mid-span deflection of all tested beams. A summary of the experimental loads and predicted loads by finite element method at the ultimate level as well as the increase in the ultimate loads based on numerical results are presented in (Table 4).*

*The highest deformation capacity was registered in the beam strengthened with inclined laminates (A10_IL). The relationship between the applied load and the deflection at mid span of the beams for FEM and experimental results are shown in (Figure 6) (Figure 7) (Figure 8) (Figure 9) and (Figure 10). It is clear from these figures there is a good agreement between the results of the experimental and FEM results using ABAQUS according to max loads. Also, (Table 4) improved this conclusion.*

***Table 4.*** *Finite element and experimental results*

| Beam designation | Experimental(EXP) | Finite element mothod(FE) | | EXP/FE |
|---|---|---|---|---|
| | Max load (KN) | Max load (KN) | Percentage Increase in Capacity (%) | (%) |
| A10-R | 100.4 | 96.2 | --- | 1.04 |
| A12-R | 116.5 | 119 | ---- | 0.98 |
| B10-R | 74.02 | 73.39 | ------ | 1.01 |
| B12-R | 75.7 | 73.36 | ------ | 1.03 |
| A10-S | 169.35 | 183.12 | 90.3 | 0.92 |
| A12-S | 215.04 | 205.5 | 72.7 | 1.04 |
| B10-S | 120.64 | 107.69 | 46.7 | 1.12 |
| B12-S | 159.10 | 154.3 | 110.3 | 1.03 |
| A10-M | 122.06 | 121.7 | 26.4 | 1.02 |
| A12-M | 179.54 | 166.48 | 39.0 | 1.07 |
| B10-M | 111.14 | 105.55 | 43.8 | 1.05 |
| B12-M | 143 | 134.35 | 83.1 | 1.06 |
| A10-VL | 158.64 | 156.4 | 62.5 | 1.01 |
| A12-VL | 235.11 | 225.02 | 87.93 | 1.04 |
| B10-VL | 131.22 | 119.36 | 62.6 | 1.10 |
| B12-VL | 139.20 | 130.65 | 78.0 | 1.06 |
| A10-IL | 157.90 | 165.39 | 72.0 | 0.95 |
| A12-IL | 262.38 | 237.60 | 99.6 | 1.10 |
| B10-IL | 120.44 | 128.85 | 75.5 | 0.93 |
| B12-IL | 148.50 | 155.32 | 111.7 | 0.95 |

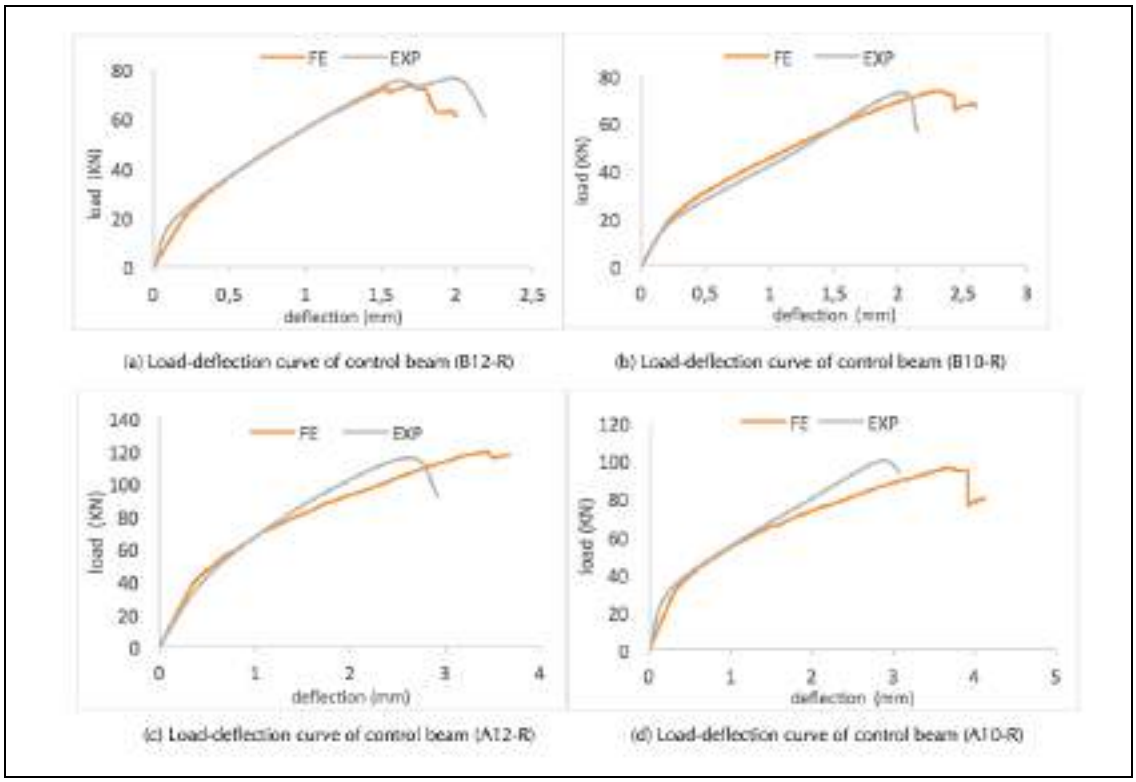


***Figure 6.*** *Load-deflection curves of control beams*

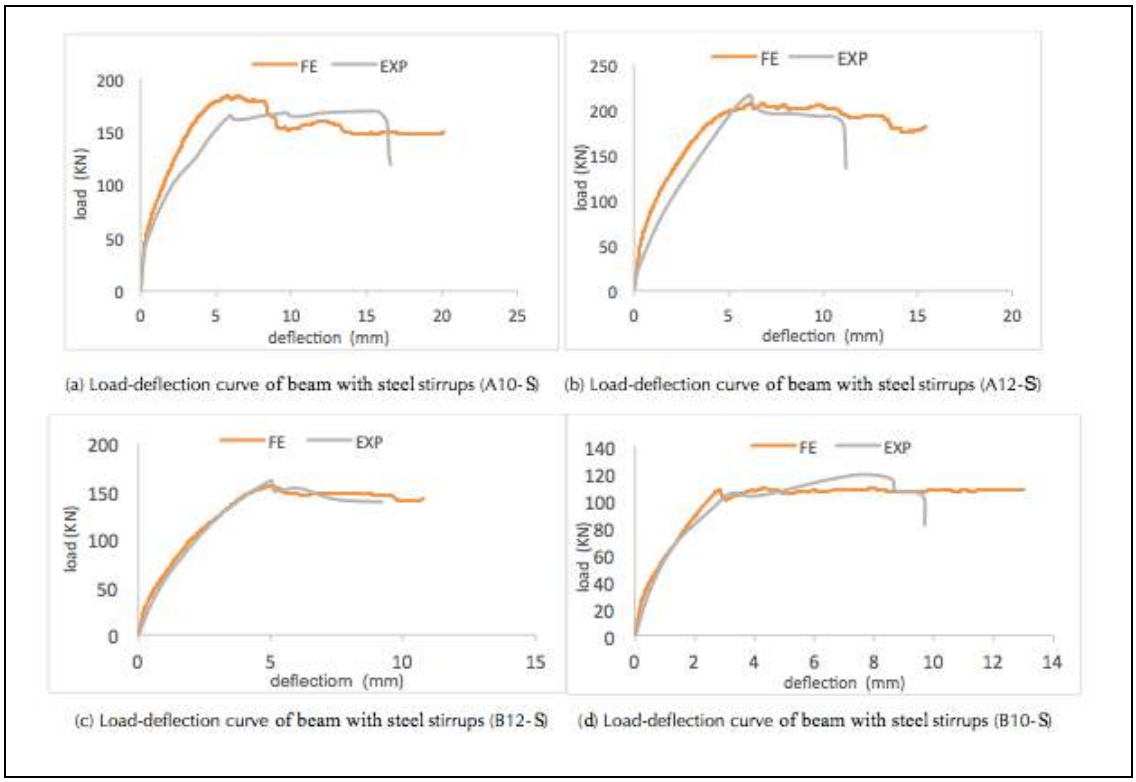


***Figure 7.*** *Load-deflection curves of beam with steel stirrups*

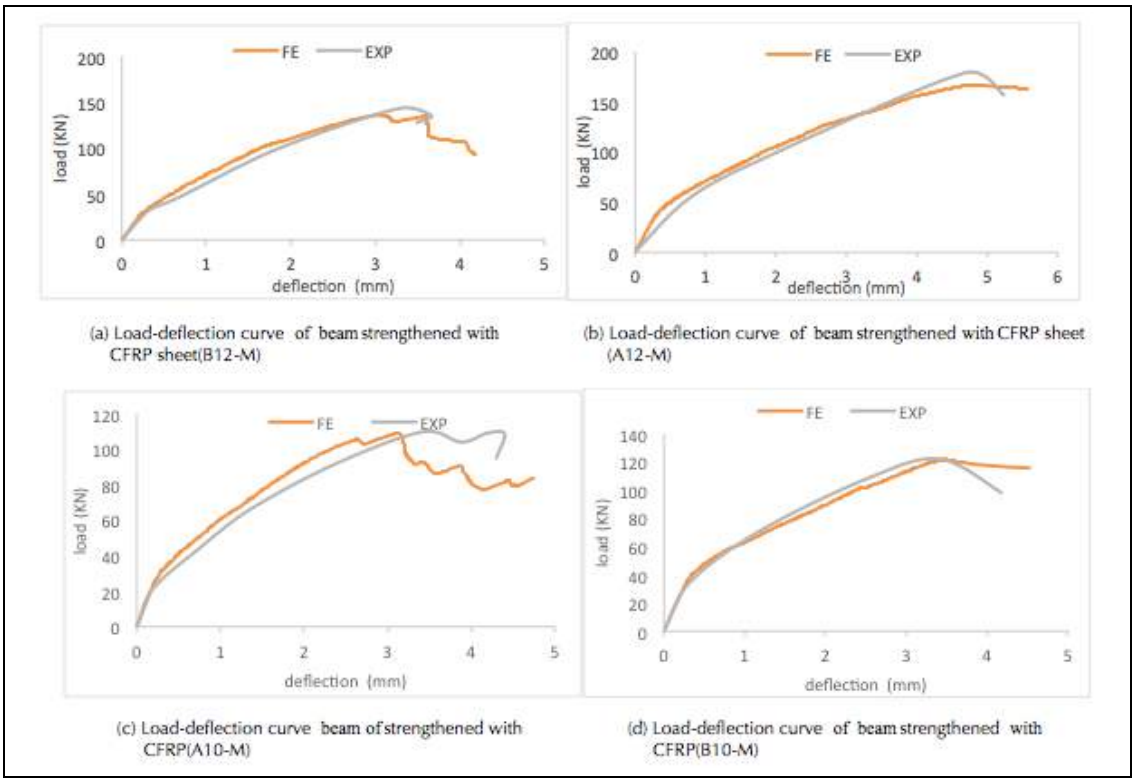


***Figure 8.*** *Load-deflection curve of beam strenghened with CFRP sheets*

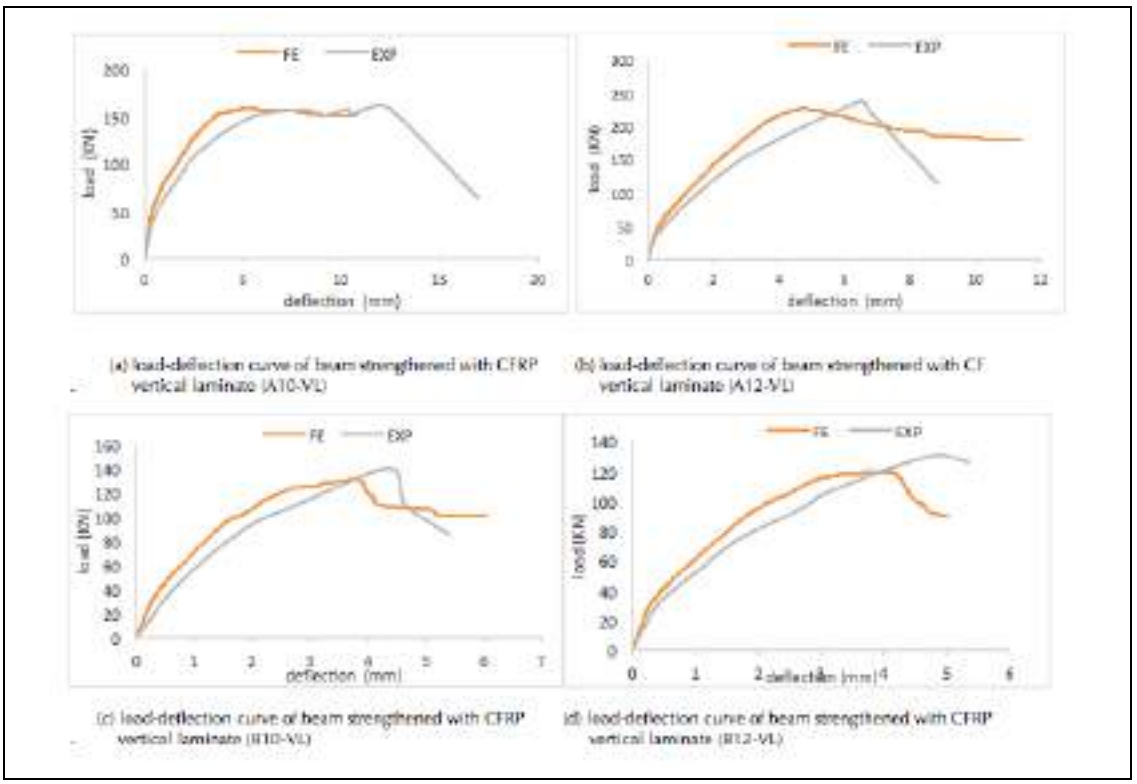


***Figure 9.*** *Load-deflection curve of beam strenghened with CFRP vertical laminate*

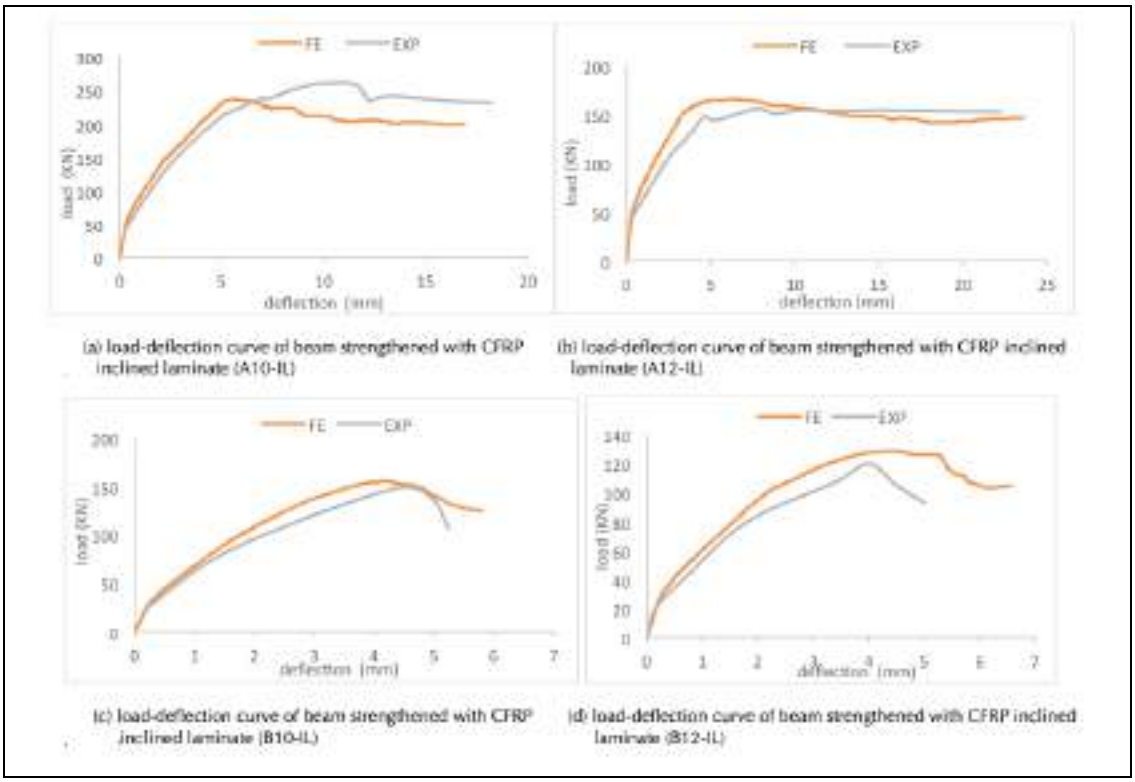


***Figure 10.*** *Load-deflection curve of beam strenghened with CFRP inclined laminate*

### *5.2 Mode failure*

*Shear failure was the failure modes of the control beams for all series (beams without shear reinforcement) and no yielding of tensile reinforcement was observed. Yielding of main steel reinforcement was observed firstly in beams A12_S and A10_S followed by shear cracks, while, shear cracks firstly occurred in beams (B10-S and B12-S) and the yielding of the longitudinal steel reinforcement was observed. Shear failure was the failure modes of beams A10-M, A12-M, B10-M, and B12-M. The shear cracks were started from compression to tension due to the U configuration of the CFRP sheets. Experimentally, the rupture of CFRP sheets was clearly observed. Conversely, no rupture was observed in the numerical results. Also, yielding of main steel reinforcement was observed firstly in beams A10_VL, and then a shear failure crack was formed. While beam A12_VL failed by shear cracks and no yielding of tensile steel was noted. The failure mode of beams B10_VL and B12_VL was forming shear cracks from load to support without yielding of longitudinal tensile reinforcement. Beams (A12_IL and A10_IL) failed by the formation of the flexural failure cracks. The mid-span deflection drops gradually after longitudinal tensile reinforcement yielded. Mode of failure of B10_IL, B12_IL beams is forming shear cracks from load to support without yielding of the longitudinal tensile reinforcement. (Figure 11) (Figure 12) (Figure 13) (Figure 14) (Figure 15) (Figure 16) (Figure 17) (Figure 18) (Figure 19) (Figure 20) (Figure 21) (Figure 22) (Figure 23) (Figure 24) (Figure 25) (Figure 26) (Figure 27) (Figure 28) (Figure 29) and (Figure 30) show the experimental and numerical failure modes of the studied beams. The ultimate load beams (A10-S, A12-S, B10-S and B12-S) at failure are higher than beams (A10-M, A12-M, B10-M, and B12-M) due to the premature FRP debonding which took place before reaching failure.*

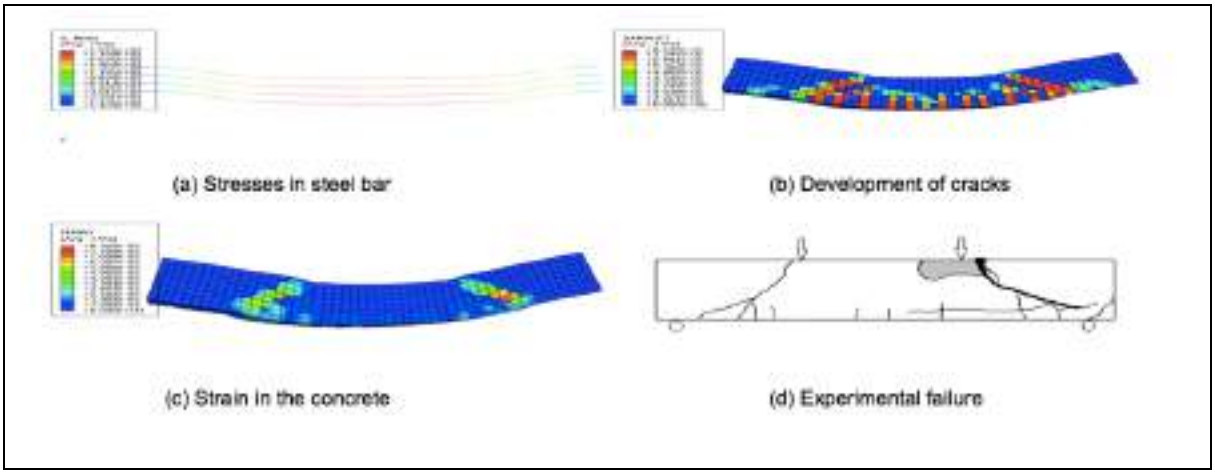


***Figure 11.*** *Mode of failure of control beaM (R B12)*

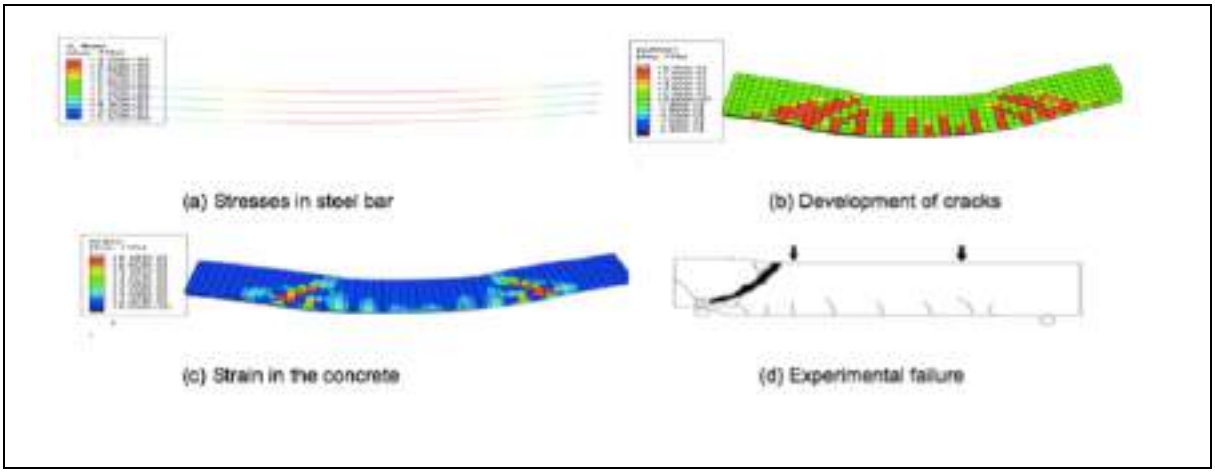


***Figure 12.*** *Mode of failure of control beam (B10-R)*

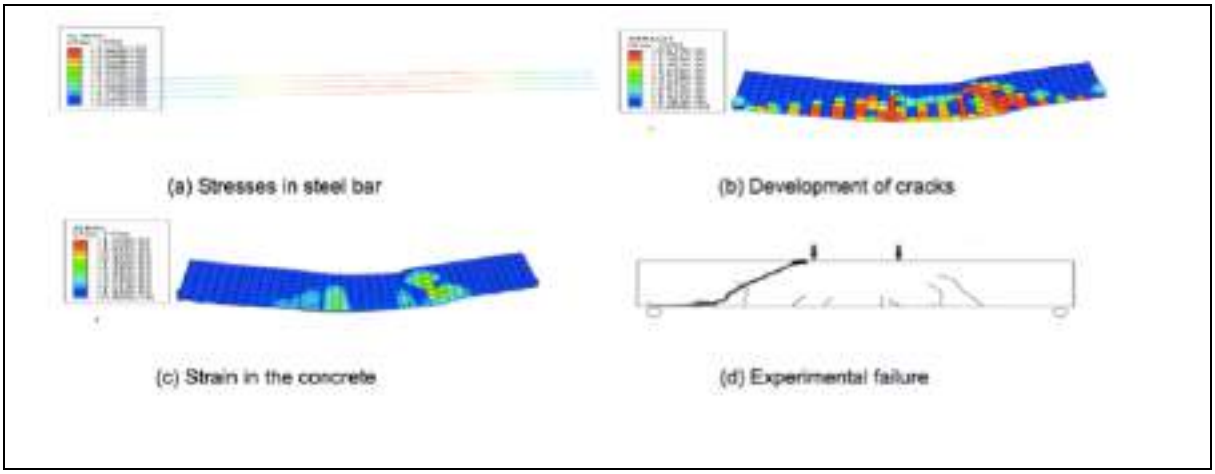


***Figure 13.*** *Mode of failure of control beam (A10-R)*

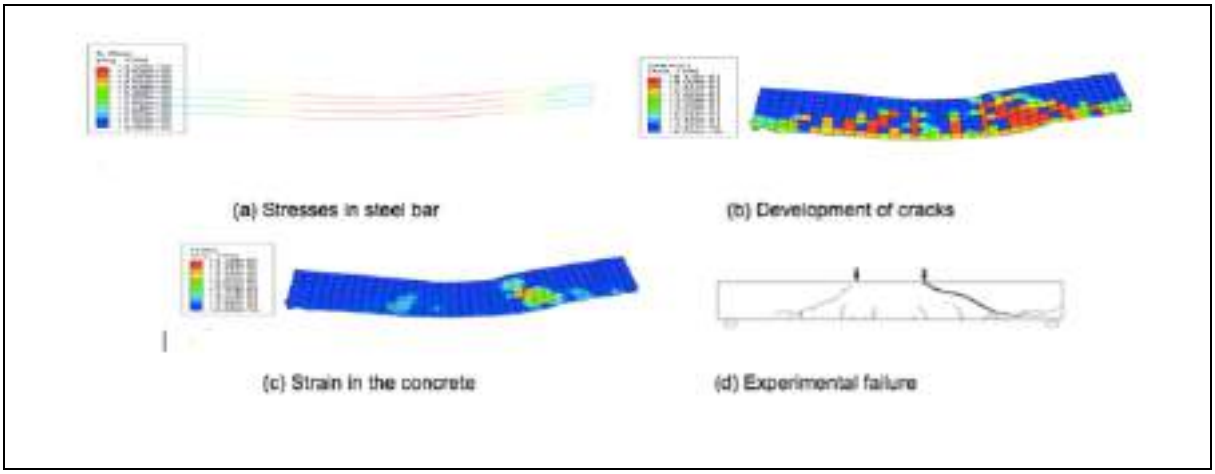


***Figure 14.*** *Mode of failure of control beam (A12-R)*

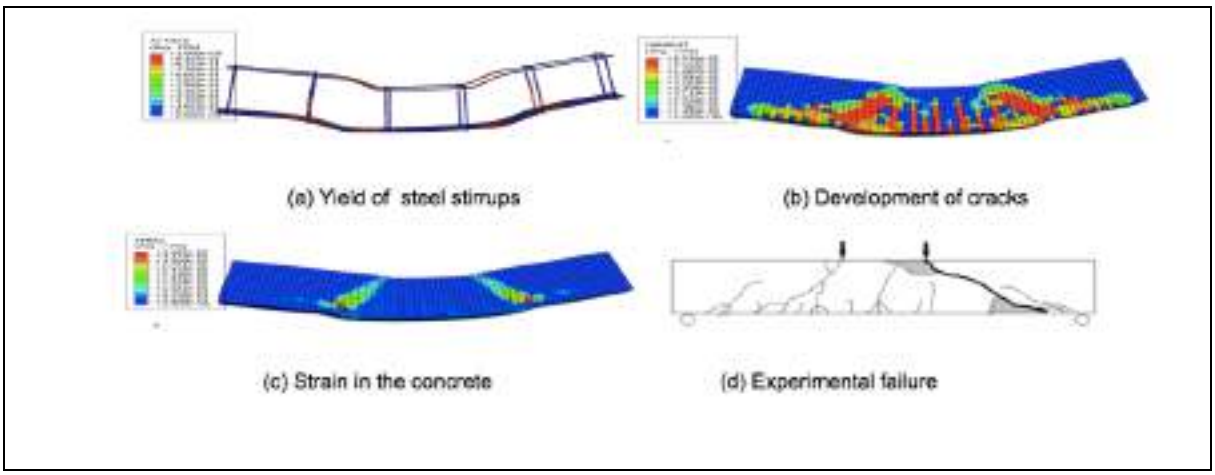


***Figure 15.*** *Mode of failure of control beam with steel stirrups (A10-S)*

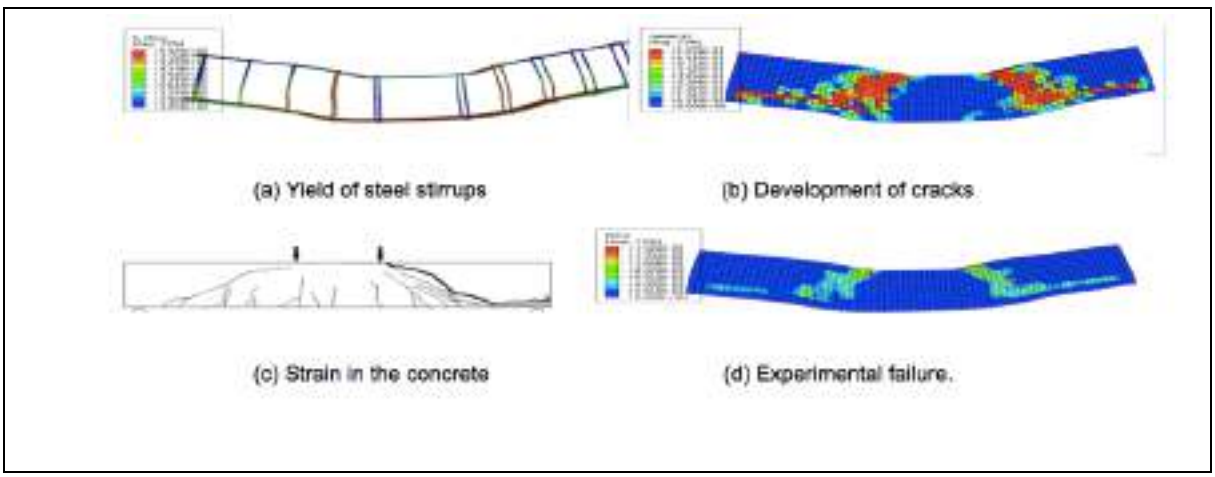


***Figure 16.*** *Mode of failure of control beam with steel stirrups (A12-S)*

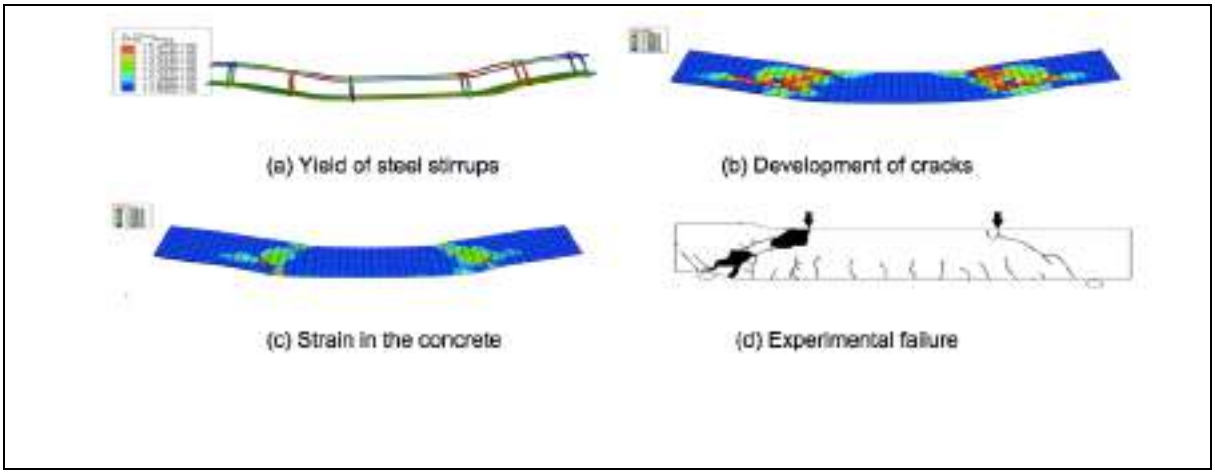


***Figure 17.*** *Mode of failure of control beam with steel stirrups (B10-S)*

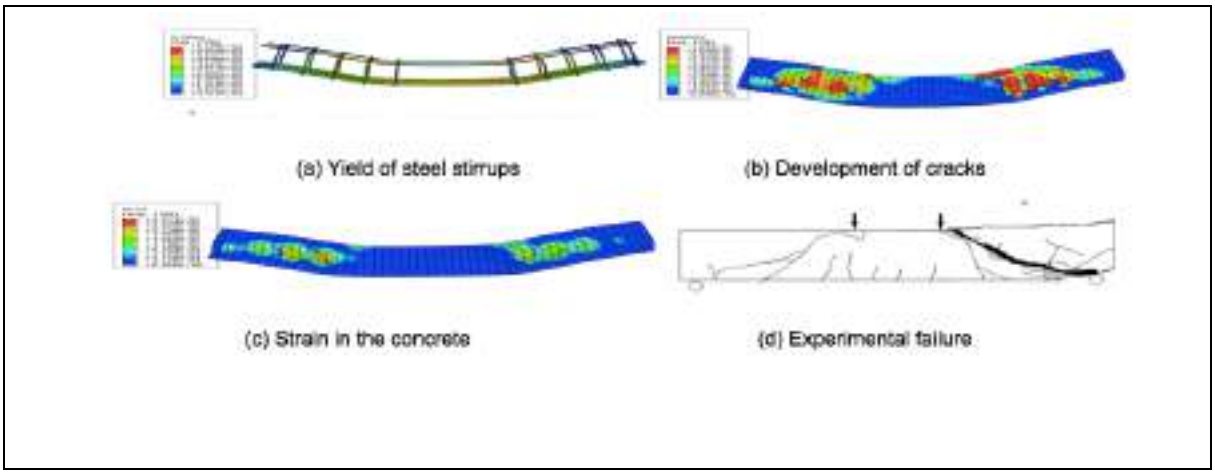


***Figure 18.*** *Mode of failure of control beam with steel stirrups (B12-S)*

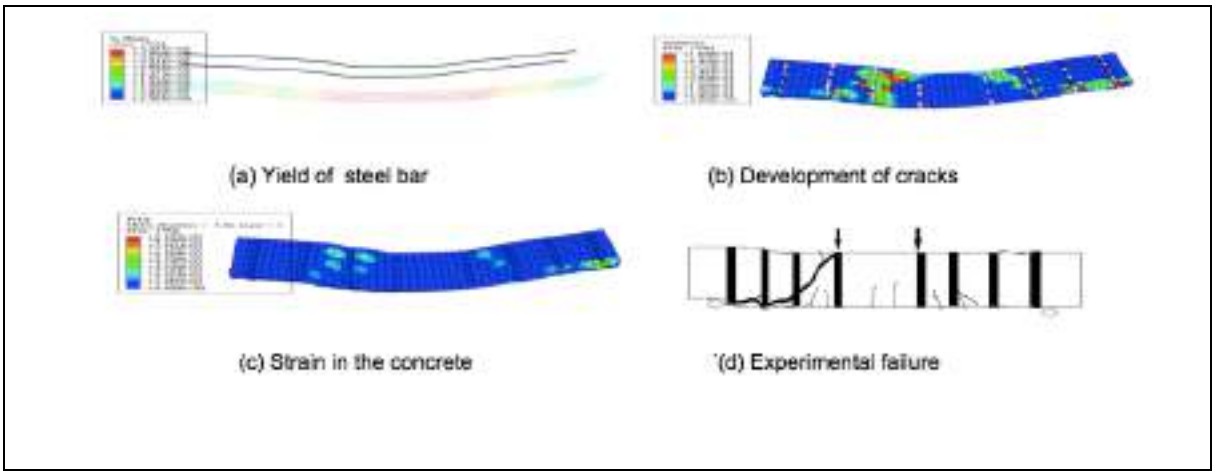


***Figure 19.*** *Mode of failure of beams strengthened with CFRP sheet (A10-M)*

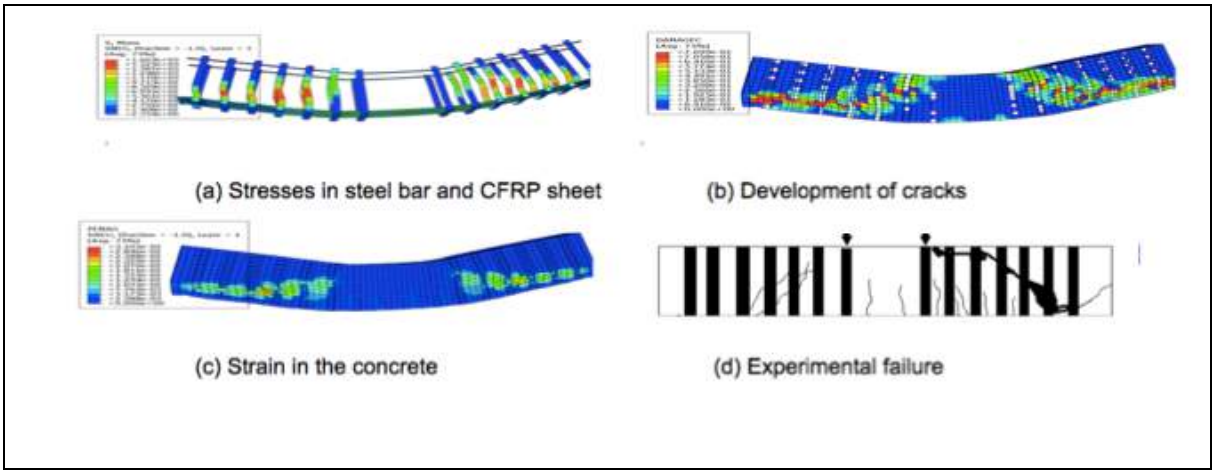


***Figure 20.*** *Mode of failure of beams strengthened with CFRP sheet (A10-M)*

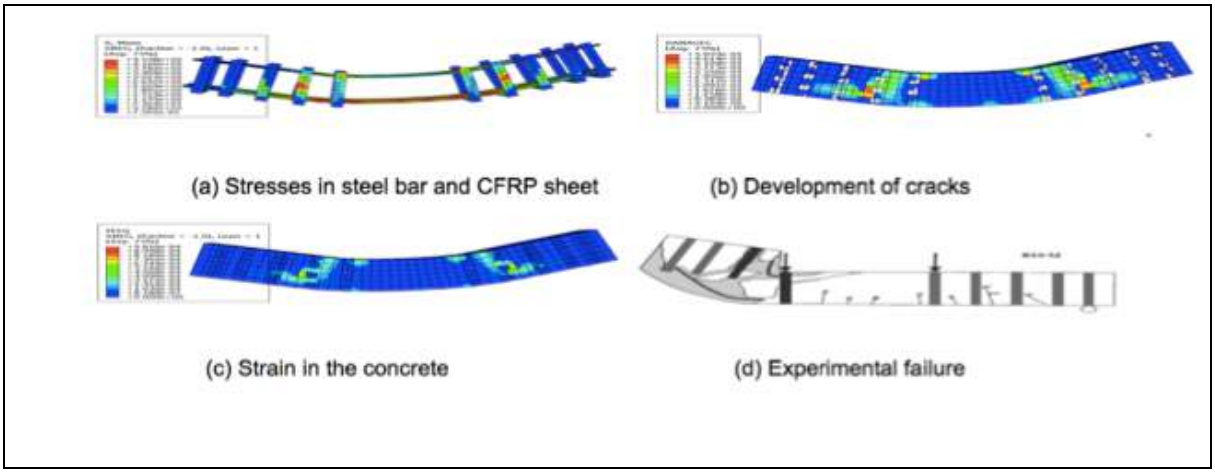


***Figure 21.*** *Mode of failure of beams strengthened with CFRP sheet (B10-M)*

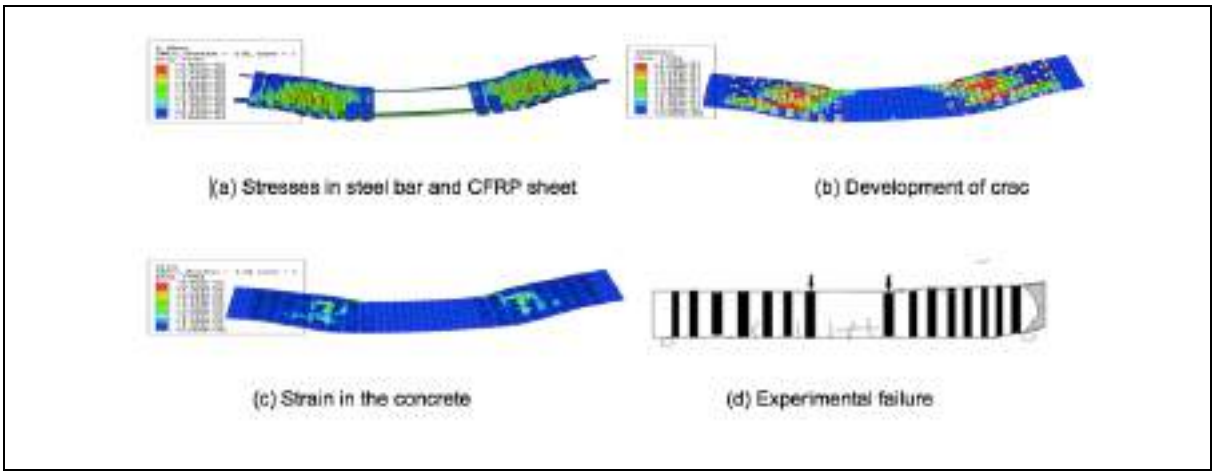


***Figure 22.*** *Mode of failure of beams strengthened with CFRP sheet (B12-M)*

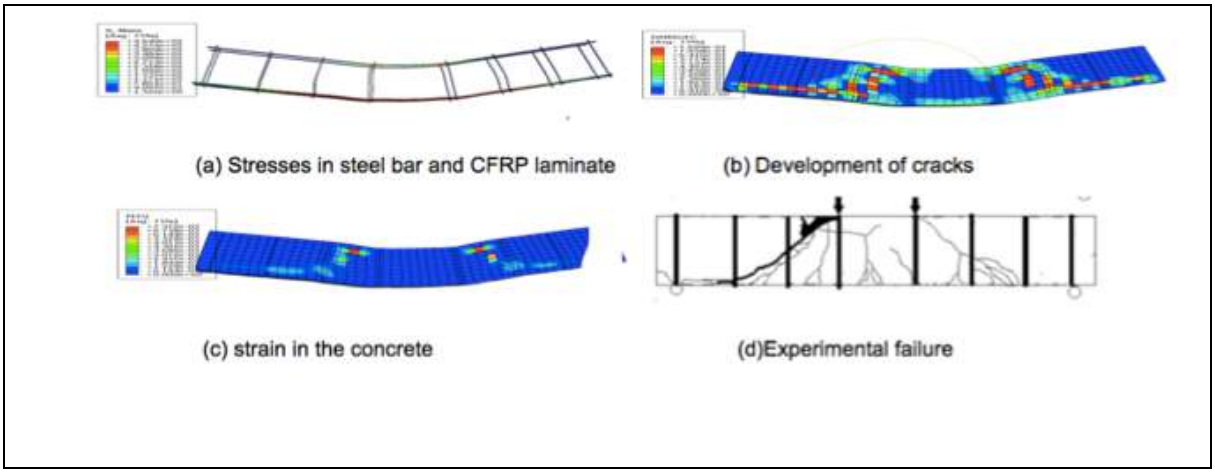


***Figure 23.*** *Mode of failure of beams strengthened with CFRP vertical laminate (A10-VL)*

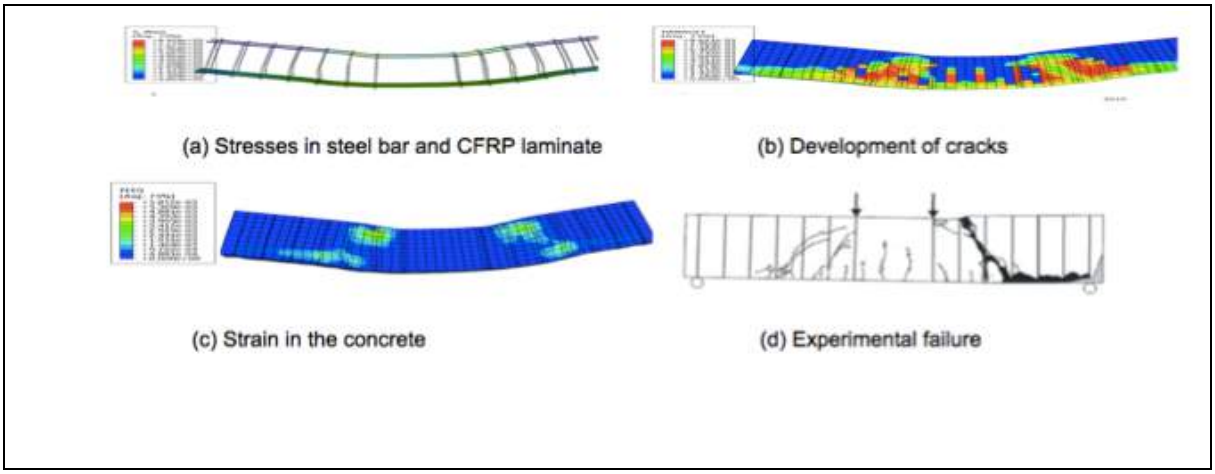


***Figure 24.*** *Mode of failure of beams strengthened with CFRP vertical laminate (A12-VL)*

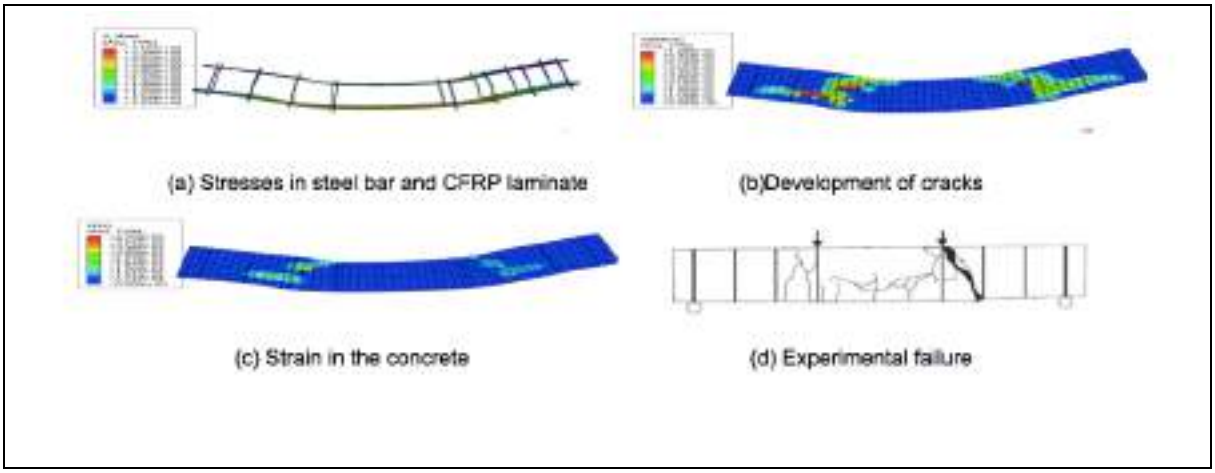


***Figure 25.*** *Mode of failure of beams strengthened with CFRP vertical laminate (B10-VL)*

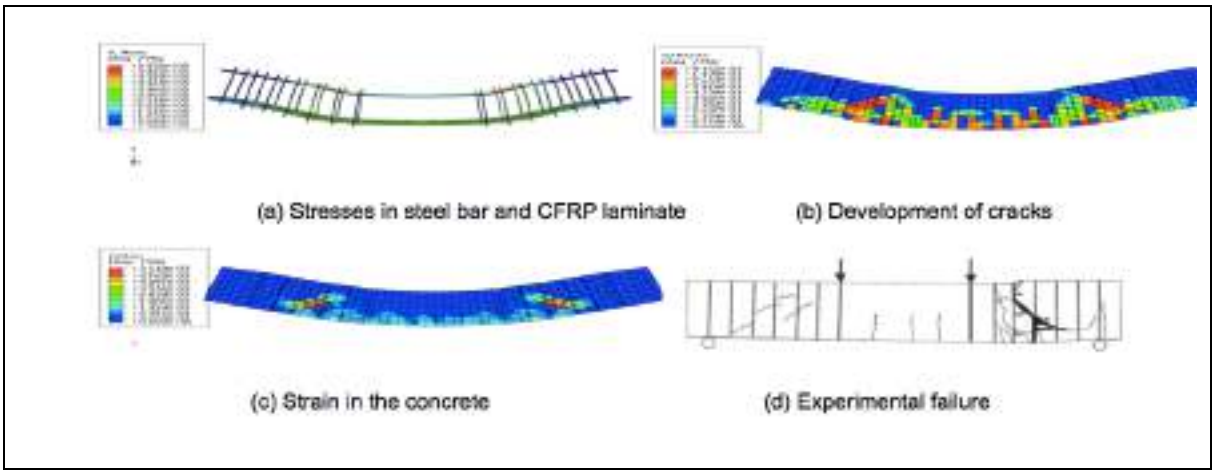


***Figure 26.*** *Mode of failure of beams strengthened with CFRP vertical laminate (B12-VL)*

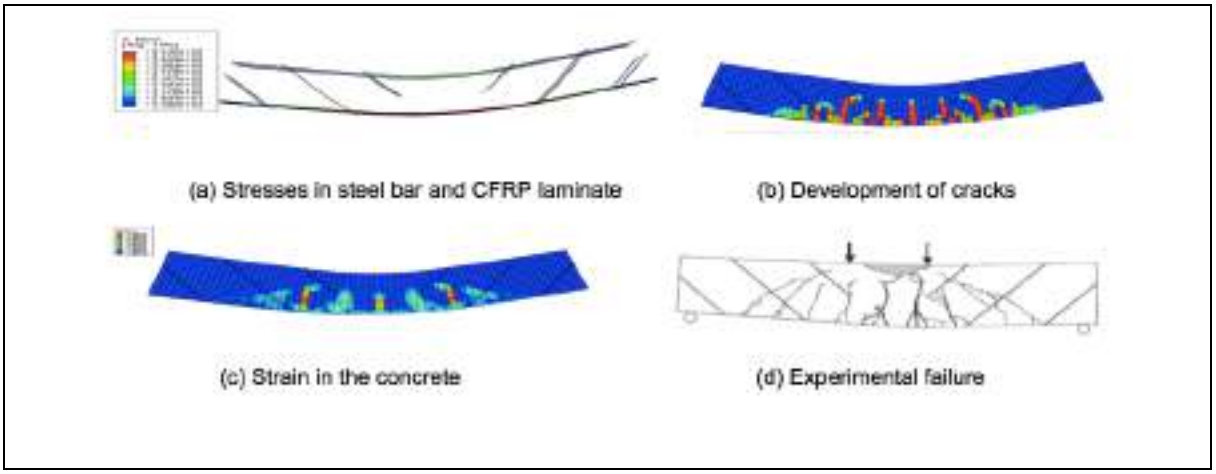


***Figure 27.*** *Mode of failure of beams strengthened with CFRP Inclined laminate (A12-IL)*

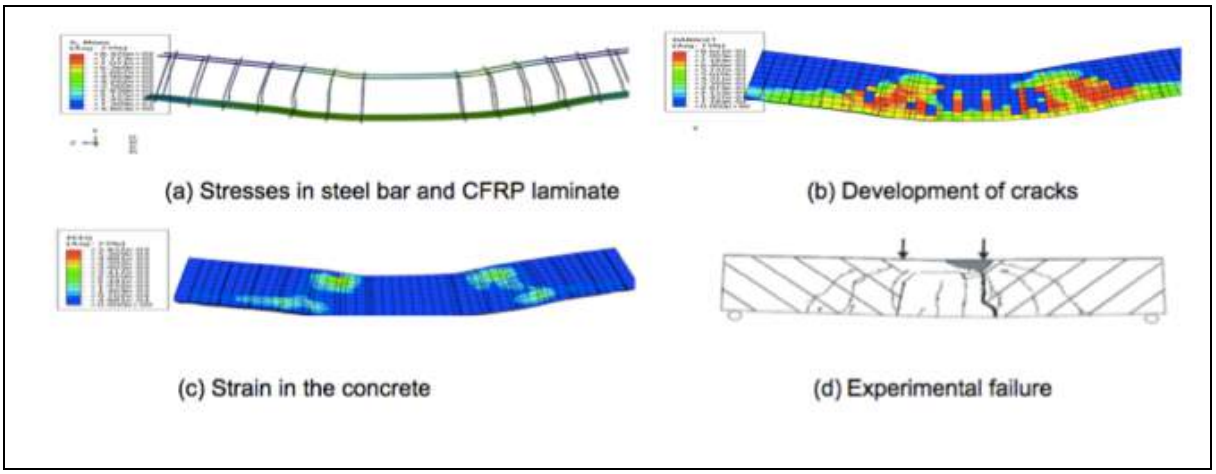


***Figure 28.*** *Mode of failure of beams strengthened with CFRP Inclined laminate (A12-IL)*

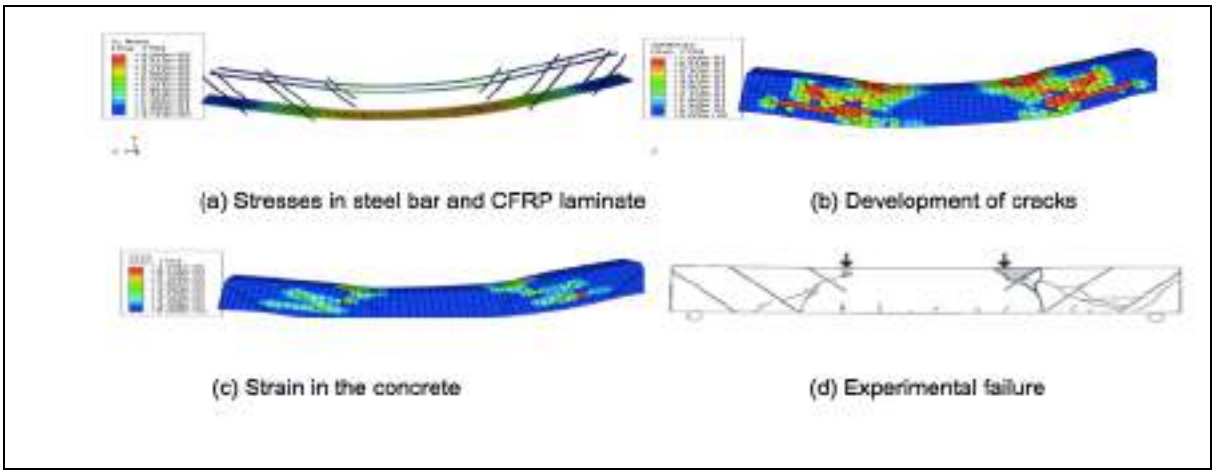


***Figure 29.*** *Mode of failure of beams strengthened with CFRP Inclined laminate (A10-IL)*

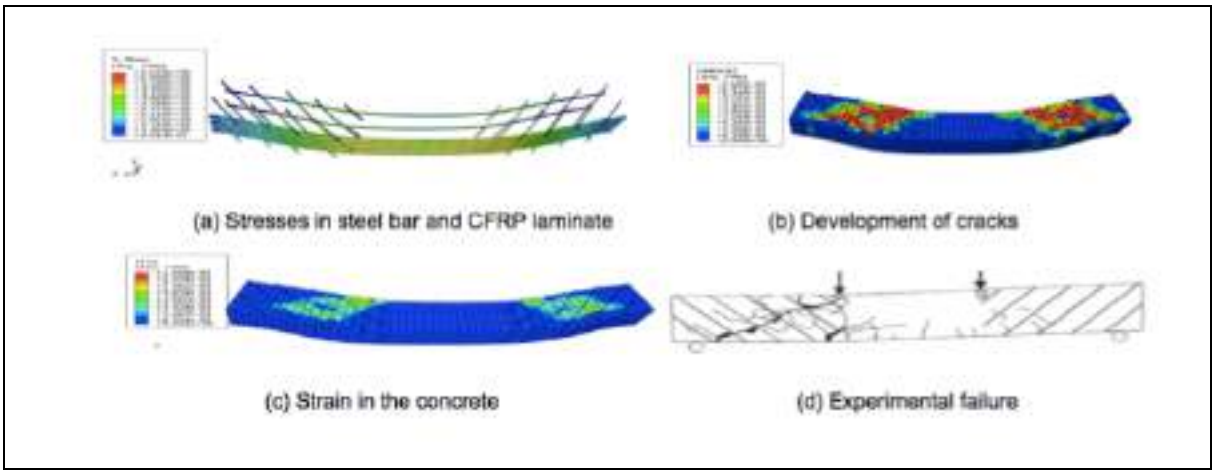


***Figure 30.*** *Mode of failure of beams strengthened with CFRP Inclined laminate (b12-IL)*

## *5.3 Parametric study*

### *5.3.1 Effect of compressive strength of concrete*

*The concrete compressive strength ($f_c'$) is an important factor that affects the shear strength and the overall behavior of the beams. The parametric study was carried out to evaluate the effects of compressive strength of concrete on the behavior strengthened beams. Twelve beams are analyzed numerically. Three values of $f_c'$ (40 MPa, 56 MPa, and 65 MPa) were considered to investigate this parameter in this study as shown in (Figure 31). The figure indicates that the stiffness and ultimate load increase as the compressive strength of concrete are increased. (Figure 32) shows the relationship between the max load and the compressive strength of concrete. Also, it is observed that the stresses in the CFRP sheet or laminite have been increases as the compressive strength of concrete increases. Beams B10-S failed by yielding of longitudinal tensile reinforcement when $f_c'$ equal to 65 MPa while no yielding was observed in beam B10-S beam with $f_c'$ 40 or 56.2 MPa. Beam B10-M failed by rupture of CFRP sheet when compressive strength equal to 65 MPa while it failed by forming shear crack without rupturing of CFRP when $f_c'$ equal to 40 and 56.2 MPa.*

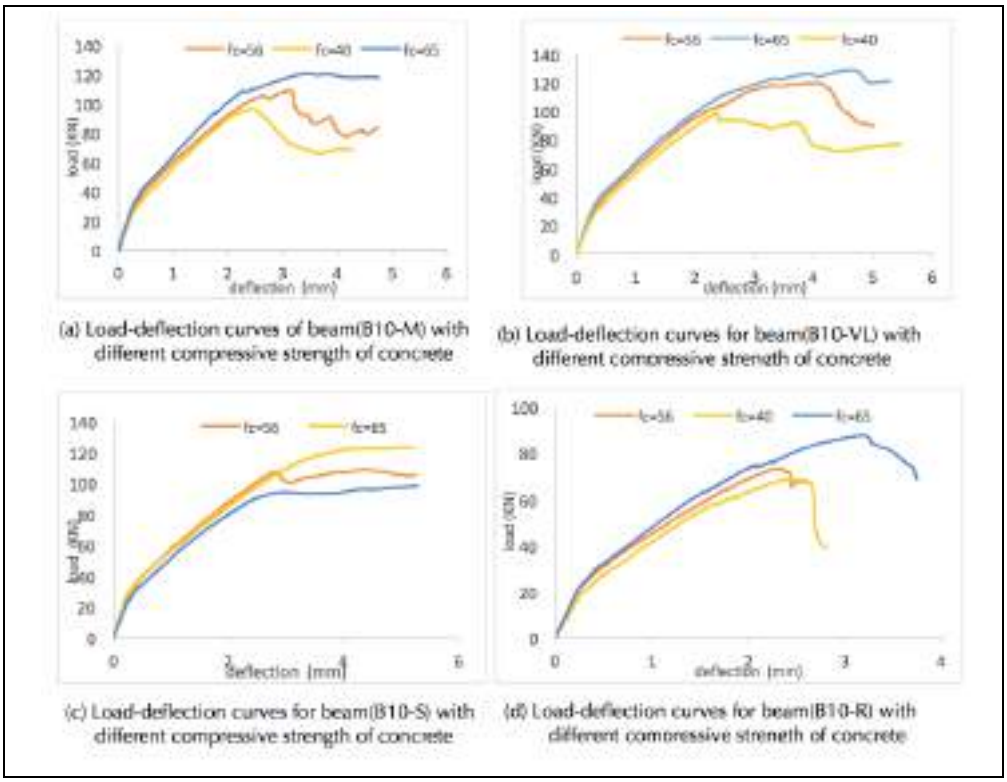


***Figure 31.*** *Load-deflection curve for different compressive strength of concrete*

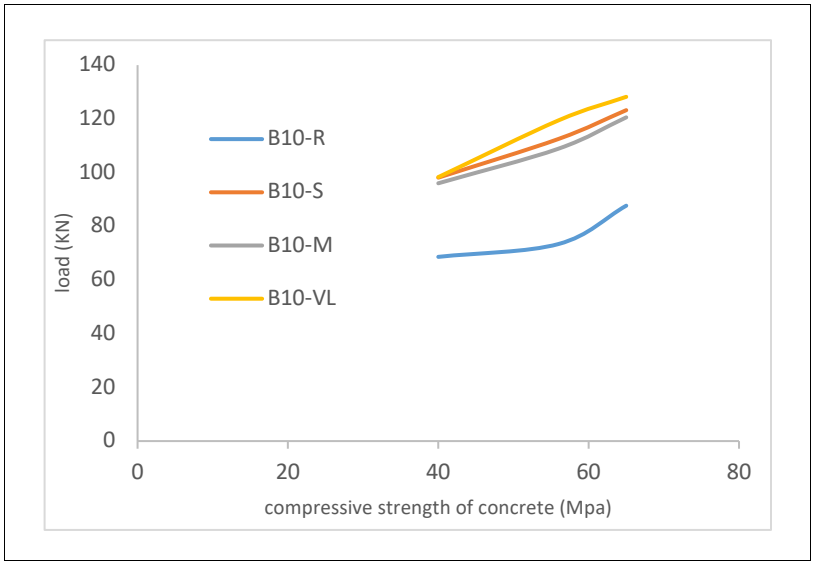


***Figure 32.*** *Relationship between load and compressive strength of concrete*

### *5.3.2 Effect of Shear span to depth ratio (a/h)*

*The a/h ratio has an essential effect on the shear behavior of RC beams. change in a/h ratio may lead to a significant change in the shear resistance. The influence of (a/h) ratio was investigated by building an FE model. Three values of a/h ratios; 1.66, 2 and 2.33 were considered. (Figure 33) and (Figure 34) show that the increase of*

*a/h ratio results in decreasing the shear strength. Shear strength decreased by about (20-30)% when increased the ratio (a/h) from 1.66 to 2.33.*

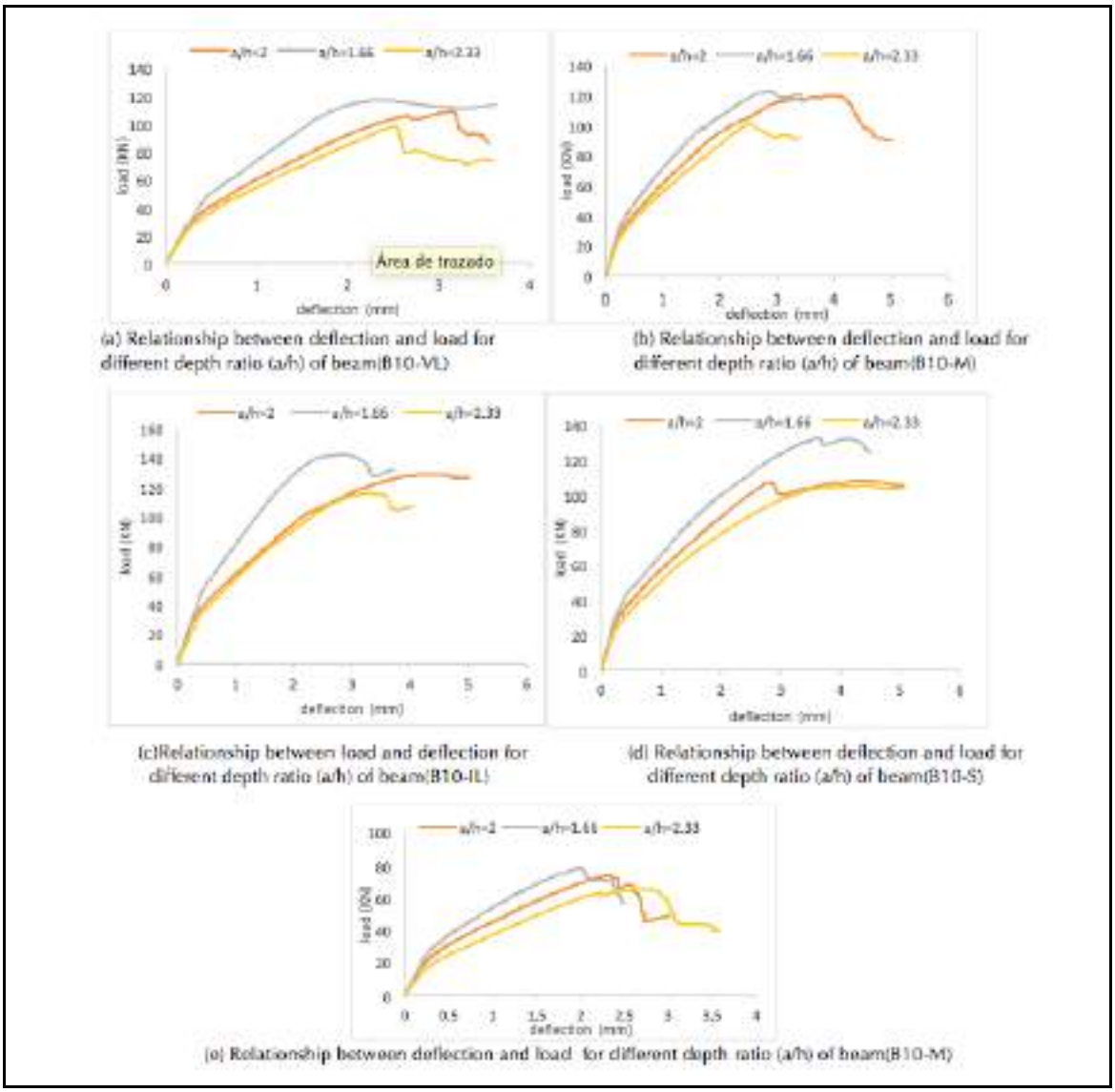


***Figure 33.*** *Relationship between load and deflection for different depth ratio (a/h)*

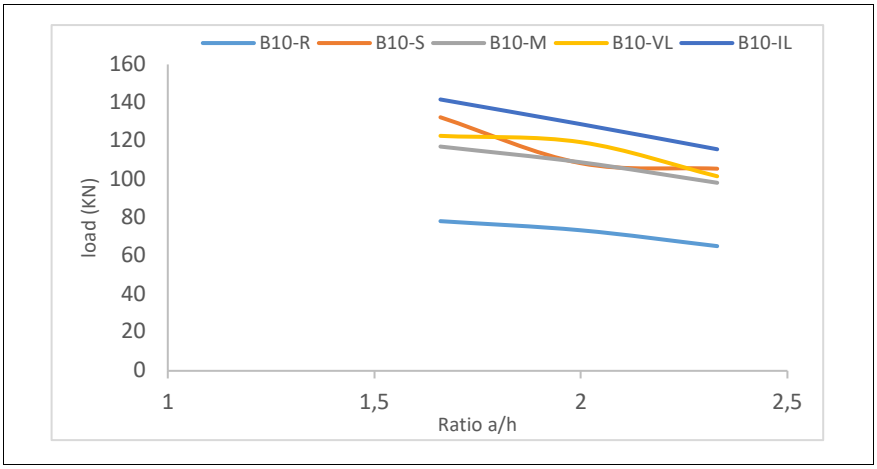


***Figure 34.*** *Relationship between max load to effect-depth ratio (a/h)*

### *5.3.3 Effect of shape of CFRP on shear strength*

*Generally, three types of CFRP wrapping schemes had been used to improve the shear strength of RC members such as beams and columns which one ( completely wrapping, U-wrap shape and two side bond shape). In this study, we used two types of strength: U shape and two side bond shapes. (Figure 35) shows that the retrofitting with U shape is slightly improves the strength of more than two sides boned. The maximum load in A10-M, A12-M, B10-M, and B12-M beams strengthened with U shape CFRP increased by 6.2%, 5.9%, 11.5%, and 9.5% respectively compared with beams retrofitted with two sides shape (figure 35).*

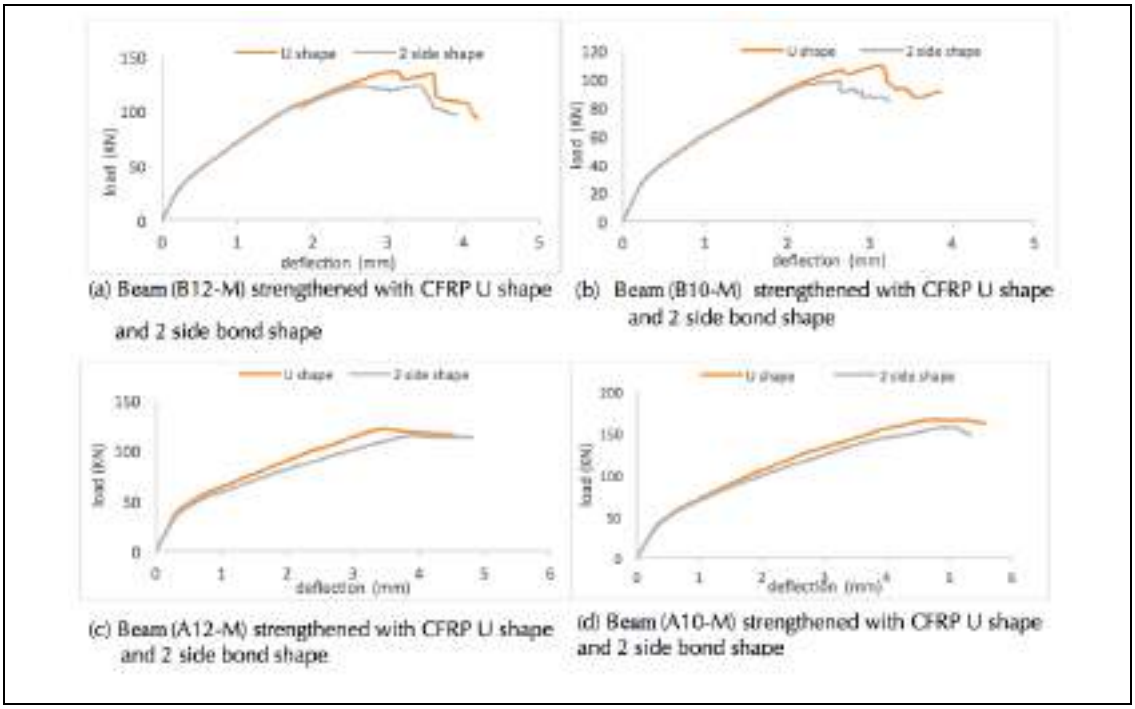


***Figure 35.*** Beams *strengthened with CFRP U shape and 2 side bond shape*

### *5.3.4 Effect of addition CFRP laminate to beams with stirrups*

*Four RC beams with traditional stirrups were strengthened by CFRP laminate to assess the effect of CFRP laminate on the strength of RC beams with stirrups (A10-S, A12-S, B10-S, and B12-S). Fig (36) shows that the capacity of beams was increased by 8.74%, 12.13%, 15.87%, and 22.73% compared with beams (A10-S, A12-S, B10-S, and B12-S) without strengthening*

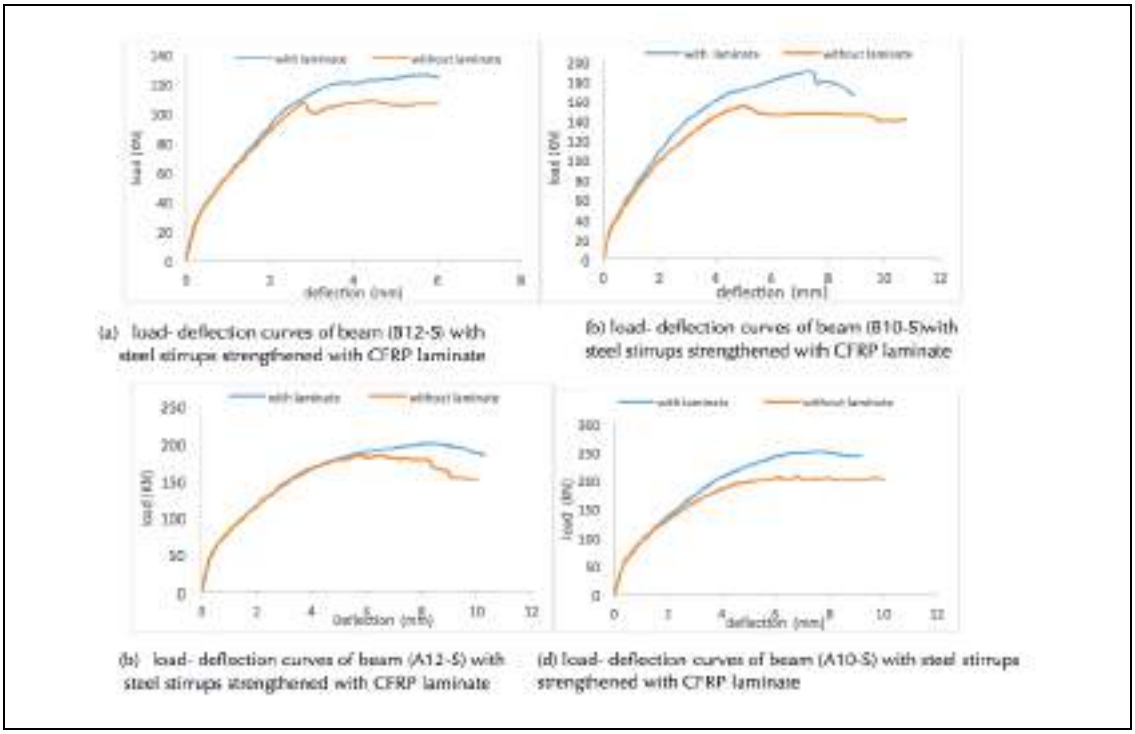


***Figure 36.*** *load- deflection curves of beams with steel stirrups strengthened with CFRP laminate*

## 6. Appraisal of the ACI-440

***Figure 35.*** Beams *strengthened with CFRP U shape and 2 side bond shape*

*According to ACI, the nominal shear strength for the beam strengthened with CFRP is calculated from the following (Equation 14):*

$$\boldsymbol{V_n = V_s + V_c + V_{ff}} \quad \textbf{(14)}$$

*(Equation 15)*

$$\boldsymbol{V_s = A_v f_y \frac{d}{S}} \quad \textbf{(15)}$$

*(Equation 16)*

$$\boldsymbol{V_c = \frac{1}{6} * \sqrt[2]{f_c^-}\, b\, d} \quad \textbf{(16)}$$

*the design value for shear strength of the CFRP is given by (Equation 17):*

$$\boldsymbol{V_{fd} = \emptyset\, \psi_f (\frac{A_{fv} f_{fe} d_f}{s_f})} \quad \textbf{(17)}$$

*for concrete material, φ has a value of 0.85, ψ f have a value for the U-wraps shape equal to 0.85 (Equation 18)*

$$\boldsymbol{A_{fv} = 2n\ t_f\, w_f} \quad \textbf{(18)}$$

*The effective stress in the FRP f fe, is obtained by multiplying the effective strain by the Young's modulus of the FRP ( Ef) (Equation 19)*

$$\boldsymbol{\varepsilon_{fe} = k_v * \epsilon_{fu} \leq 0.004} \quad \textit{(19)}$$

*where (Equation 20):*

$$\boldsymbol{k_v = \frac{k_1 k_2 L_e}{11900 \varepsilon_{fu}} \leq 0.75} \quad \textit{(20)}$$

*where (Equation 21):*

$$\boldsymbol{L_e = (23300)/(nt_f E_f)^{0.58}} \quad \textit{(21)}$$

*(Equation 22)*

$$\boldsymbol{k_1 = (\frac{f_c^-}{27})^{2/3}} \quad \textit{(22)}$$

*(Equation 23)*

$$\boldsymbol{k_2 = \frac{d_f - L_e}{d_f}} \quad \textit{(23)}$$

*In (Equation 10) and (Equation 4) $d_f$ is the effective depth of the beam. $f_c^-$ is the concrete compressive strength. The force and the length unities of the variables in (Equation 7) (Equation 8) (Equation 9) and (Equation 10) are Newton and millimeter respectively. (Table 5) shows the results for finite element method, experimental and ACI of RC beams in shear behavior and compared between them.*

***Table 5.*** *Finite element method (FEM), ACI and Experimental results*

| Beam designation | FEM | ACI | Experimental | EXP/ACI | FE/ACI |
|---|---|---|---|---|---|
| | Maximum load (KN) | Maximum load (KN) | Maximum load (KN) | | |
| A10-R | 96.2 | 77.5 | 100.40 | 1.3 | 1.24 |
| A12-R | 119 | 77.28 | 116.50 | 1.5 | 1.53 |
| B10-R | 73.39 | 35.04 | 74.02 | 2.11 | 2.09 |
| B12-R | 73.36 | 34.82 | 75.70 | 2.17 | 2.1 |
| A10-S | 183.12 | 122.46 | 169.35 | 1.38 | 1.49 |
| A12-S | 205.5 | 166.86 | 215.04 | 1.29 | 1.23 |
| B10-S | 107.69 | 73.08 | 120.64 | 1.65 | 1.47 |
| B12-S | 154.3 | 110.22 | 159.10 | 1.44 | 1.34 |
| A10-M | 121.7 | 115.82 | 122.06 | 1.05 | 1.05 |
| A12-M | 166.48 | 153.66 | 179.54 | 1.17 | 1.08 |
| B10-M | 105.55 | 73.46 | 111.14 | 1.51 | 1.43 |
| B12-M | 134.35 | 111.04 | 143.00 | 1.29 | 1.21 |

## 7. Conclusions

1. *The good agreement between FEM and experimental results for the RC beams strengthened with CFRP laminate or sheet. The maximum difference between the experimental and analytical results is 12%.*
2. *Strengthening of RC beams for shear using CFRP sheet or laminate improves the load-carrying capacity of the RC beams up to 117.7%, in this study.*
3. *Strengthening RC beams using either U shape wrapped or 2-side bond shape is very important to increase the shear strength. The U shape wrapped beam is more efficiency in increasing the ultimate load and stiffness than the 2-side bond shape. The maximum load of beams strengthened with U shape was increased by 5.9% to 11.5% for beams strengthened by CFRP sheet, A12-M and B10-M respectively when compared with the same beams strengthened with two-side bond shape of CFRP.*
4. *The different between FEM results and experimental results is 12%, while the difference between FEM and ACI 440.1R-17 approach reached 109%. Also, the difference between experimental and ACI 440.1R-17 approach reached 217%, this indicates that the finite element method (FEM) is a very good tool to predicate the shear strength of CFRP-RC beams.*
5. *The crack patterns and modes failure obtained from the FE models and the experimental work, in general, are similar.*
6. *The decrease of shear span to depth ratio (a/h) from 1.66 to 2.33 leads to increasing the load carrying capacity by 23%.*
7. *The NSM was the most efficient of the CFRP systems than EBR in shear strengthening.*
8. *This research shows the potential of FE as a method to support the structural field problems in the modeling of shear of CFRP- reinforced concrete beams and developing a parametric study to assess the effect of each parameter on the shear of CFRP- reinforced concrete beams. Therefore, it is considered that the application of the finite element method may provide a simple method for most problems in structural engineering fields.*

***Funding***
*This research received no external funding.*

***Conflicts of Interest***
*The authors declare no conflict of interest.*

## 8. References

**Al Rjoub, Y.S., et al. (2019).** Shear strengthening of RC beams using near-surface mounted carbon fibre-reinforced polymers. Australian Journal of Structural Engineering, 20(1): p. 54-62.DOI: https://doi.org/10.1080/13287982.2019.1565617

**Barros, J.A.; Dias, S.J.; Lima, J.L. (2007).** Efficacy of CFRP-based techniques for the flexural and shear strengthening of concrete beams. Cement and Concrete Composites, 29(3): p. 203-217.DOI: https://doi.org/10.1016/j.cemconcomp.2006.09.001

**CEN. European Committee for Standarization (2004).** 1992-1-1, E. Design of concrete structures - Part 1-1: General rules and rules for buildings. Brussels: CEN.

**Chen, W., et al. (2018).** Experimental study of flexural behaviour of RC beams strengthened by longitudinal and U-shaped basalt FRP sheet. Composites Part B: Engineering, 134: p. 114-126. DOI: https://doi.org/10.1016/j.compositesb.2017.09.053

**de Normalisation, C.E. (2004).** Design of concrete structures—Part 1-1: General rules and rules for buildings. Eurocode 2, EN 1992-1-1: E, 2004.DOI: https://www.phd.eng.br/wp-content/uploads/2015/12/en.1992.1.1.2004.pdf

**Guo, Z., et al. (2005).** Experimental study on bond stress-slip behaviour between FRP sheets and concrete. in FRP in construction, proceedings of the international symposium on bond behaviour of FRP in structures. DOI: https://www.researchgate.net/profile/Serge_Shilko/post/how_to_study_slip_and_interface_effects_of_steel_confined_composite_beams_under_flexure/attachment/59d6280779197b807798662a/AS:328343963619331@1455294709660/download/Experimental+Study+on+Bond+Stress-Slip+Behaviour+between+FRP+Sheets+and+Concrete.pdf

**Hibbitt, K.; Sorensen, Inc. (2000).** ABAQUS theory manual. 2000, Pawtucket, USA: Hibbitt, Karlsson & Sorensen, Inc.

**Ibrahim, A.M.; Mahmood, M.S. (2009).** Finite element modeling of reinforced concrete beams strengthened with FRP laminates. European Journal of Scientific Research, 30(4): p. 526-541.DOI:https://www.researchgate.net/profile/Mohammed_Mahmood2/publication/242163873_Finite_Element_Modeling_of_Reinforced_Concrete_Beams_Strengthened_with_FRP_Laminates/links/54ac15a60cf2bce6aa1df984/Finite-Element-Modeling-of-Reinforced-Concrete-Beams-Strengthened-with-FRP-Laminates.pdf

**Jain, R.; Lee, L. (2012).** Fiber reinforced polymer (FRP) composites for infrastructure applications: focusing on innovation, technology implementation and sustainability. Springer. DOI: https://link.springer.com/content/pdf/10.1007/978-94-007-2357-3.pdf

**JCI. (1998).** Technical report on retrofit technology for concrete structures., in Technical committee on retrofitting technology for concrete structures. p. 24-116.

**JCI. (2003).** Technical report on retrofit technology for concrete structures, in Technical committee on retrofitting technology for concrete structures. p. p. 79–97.

**Kadhim, M.M.; Adheem, A.H.; Jawdhari, A.R. (2019).** Nonlinear Finite Element Modelling and Parametric Analysis of Shear Strengthening RC T-Beams with NSM CFRP Technique. International Journal of Civil Engineering, 17: p. 1295–1306. DOI: https://link.springer.com/article/10.1007/s40999-018-0387-8

**Lee, T.K.; Al-Mahaidi, R. (2008).** An experimental investigation on shear behaviour of RC T-beams strengthened with CFRP using photogrammetry. Composite Structures, 82(2): p. 185-193. DOI: https://doi.org/10.1016/j.compstruct.2006.12.012

**Lu, X., et al. (2005).** Bond–slip models for FRP sheets/plates bonded to concrete. Engineering structures, 27(6): p. 920-937.DOI: https://doi.org/10.1016/j.engstruct.2005.01.014

**Mabrouk, A.G.; Ramadan, aO.M. (2017).** Finite element modeling of RC beams strengthened with side bonded CFRP sheet. APFIS2017 - 6th Asia-Pacific Conference on FRP in Structures. Singapore DOI: https://www.iifc.org/proceedings/APFIS_2017/Conference%20Proceedings/All%20papers/P166.pdf

**Mostofinejad, D.; Esfahani, M.R.; Shomali, A. (2019).** Experimental and numerical study of the RC beams shear-strengthened with NSM technique. Journal of Composite Materials, 53 (17):2377-2389 p. 0021998319830777.DOI: https://doi.org/10.1177%2F0021998319830777

**Obaidat, Y.T.; Dahlblom, O.; Heyden, S. (2010).** Nonlinear FE modelling of shear behaviour in RC beam retrofitted with CFRP. In: Computational Modelling of Concrete Structures : EURO-C 2010. CRC Press. DOI: https://www.researchgate.net/profile/Fatimah_Naser/post/How_we_can_apply_FRP_in_Concrete_beam_with_Abaqus/attachment/5ae88996b53d2f63c3c92b68/AS%3A621501925576707%401525189014697/download/Abaqua.pdf#page=57

**Rodríguez G., J; Bonilla J.; Hernández J, (2016).** Numerical modeling of reinforced concrete continuous deep beams Revista Ingeniería de Construcción, 31(3):p: 163-174.

**Yu, F., et al. (2019).** Experimental study on high pre-cracked RC beams shear-strengthened with CFRP strips. Composite Structures, 225. p. 111-163. DOI: https://doi.org/10.1016/j.compstruct.2019.111163.